DRDC-RDDC-2015-P107

Improved SAR-GMTI via Optimized Cramér-Rao Bound

Christoph H. Gierull, Ishuwa Sikaneta, Defence R&D Canada (DRDC), Ottawa Research Center, Canada
Delphine Cerutti-Maori, Fraunhofer Institute for High Frequency Physics and Radar Techniques (FHR), Germany

Abstract

This paper presents a theoretical study on an optimum SAR-GMTI mode that exploits the flexible programmability of modern phased array radars such as RADARSAT-2 (R2) and TerraSAR-X. One major challenge for SAR-GMTI is the considerable re-positioning error owing to large stand-off ranges. A new GMTI mode is proposed that combines the two concepts of *antenna tapering* with *aperture switching* between subsequent transmit (Tx) pulses. The suitable antenna taper is determined via global minimization of the Cramer-Rao-Bound (CRB) of a new generalized signal model in the Doppler domain. We show that the new mode outperforms existing GMTI modes on R2 albeit trading it off with some (acceptable) SNIR loss.

1 Introduction

SAR-GMTI is part of the R2 mission through the Moving Object Detection EXperiment (MODEX) [1]. In the classic two-channel GMTI mode MODEX-1 the full antenna transmits and the echo signal is recorded in parallel on the right and left antenna wing. After launch of R2, innovative new modes (MODEX-2) have been added on-board the spacecraft that cyclically turn-off different parts of the Tx or receive (Rx) antennas between pulses [2]. Three different schemes for two subsequent pulses are shown in **Fig. 1**. Each colored box depicts either (orange) the active Tx apertures or (blue) the active Rx apertures, where the hinted sensor symbols describe the individual phase centers (black) and the resulting two-way ones (blue). Evidently, MODEX-2 provides more than two phase centers which have been proven to significantly improve GMTI capabilities [3], in particular the target location accuracy. Nevertheless, the question whether there exist even better partitions has not been answered yet. More generally, we want to find all TR-module attenuators and phase shifter settings for two subsequent pulses (which are cyclically repeated) that yield optimum performance, Fig. 1 bottom right.

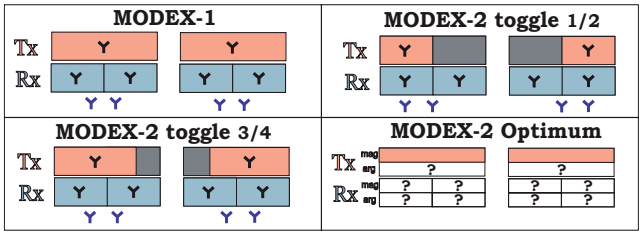

Figure 1: RADARSAT-2 MODEX modes.

Optimum SAR-GMTI in general is twofold, a) find techniques that maximize the probability of detection (aka the SNIR) and b) find target parameter estimators that reach the Cramer-Rao-Bound (CRB). In reality, however, it has been shown that it is virtually impossible to optimize both criteria simultaneously as they trade off against each other [2]. Nevertheless, for specific radar systems it is desirable to find optimum antenna configurations that minimize the CRB while preserving a favorable SNIR. In many applications with large stand-off ranges, the entire available target energy along the synthetic aperture must be integrated to achieve sufficient target SNR [3].

2 General Signal model

Consider a linear array antenna with N-TR-modules measuring the impinging backscattered wavefield, e.g. $N = 16$ for R2; black triangles in **Fig. 2**. The array is mounted in flight direction onto a platform that moves with velocity v_a into the x-direction. The element positions are denoted x_n.

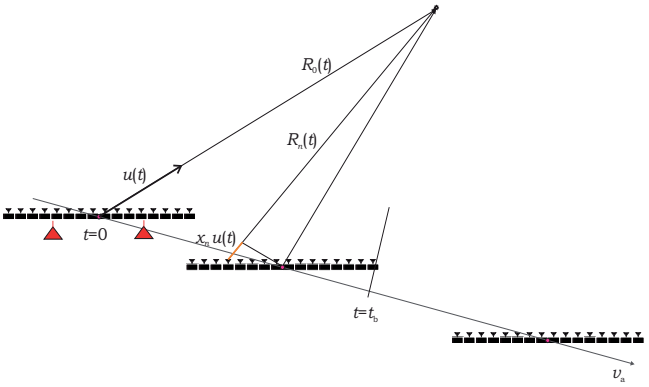

Figure 2: Range and direction time history of a moving antenna array.

Note, these spatial samples are in the RF-domain and not directly recorded, i.e. accessible by a signal processor. In other words, subsets of the RF-outputs are commonly combined and fed to a small number of parallel Rx channels containing amplification, sampling and A/D-conversion. R2, for instance, combines the eight

outputs of either wing to its two parallel Rx channels, which in Figure 2 are depicted by red triangles.

If we denote the complex Tx and Rx antenna characteristics of the n-th antenna element in direction u (at center frequency) by $D_{t,n}\big(u(t)\big)$, and $D_{r,n}\big(u(t)\big)$, respectively, the multi-channel signal model reads:

$$\mathbf{s}(t) = a\Big(e^{-j2kR_n(t)}\, D_{t,n}\big(u(t)\big)\, D_{r,n}\big(u(t)\big)\Big)_{n=1,\ldots,N}, \tag{1}$$

where $a \in \mathbb{C}$ is the amplitude describing the reflectivity of the scatterer, $R_n(t)$ denotes the range to the n-th channel, and $k = 2\pi/\lambda$ is the wavenumber. Without loss of generality we will focus on the directional cosine u, i.e. the projection of $\vec{u}$ onto the antenna array axis $\vec{x}$. The parameters describing the moving target are the constant velocities in along-track direction v_x, in across-track direction v_y, and its location x_b at broadside time $t = t_b$ which are combined in the vector $\boldsymbol{\xi} = [a, v_x, v_y, t_b]'$. The range-position y_b is assumed to be known because of the range-resolution of the radar. Assuming an equidistant spacing of d between the elements and that the far field condition is satisfied, the range from the n-th element to the moving target is given to $R_n(t, \boldsymbol{\xi}) \cong R_0(t) + n\, u(t, \boldsymbol{\xi})\, d/2$, where the common range term for all elements is

$$R_0(t, \boldsymbol{\xi}) \cong R_b + v_s(t - t_b) + \frac{v_{\text{rel}}^2}{2R_b}(t - t_b)^2, \tag{2}$$

with $v_s = \frac{y_b}{R_b} v_y$ and $v_{\text{rel}}^2 = (v_x - v_a)^2 + v_s^2$. The broadside distance is denoted as R_b. Equivalently, the series expansion of u up to second order yields $u(t, \boldsymbol{\xi}) \simeq \frac{v_x - v_a}{R_b}(t - t_b)$. Inserting this into (1) yields the vector valued signal:

$$\mathbf{s}(t, \boldsymbol{\xi}) = a e^{-j2kR_0(t - t_b, \boldsymbol{\xi})}\, \mathbf{d}\big(u(t - t_b, \boldsymbol{\xi})\big) \quad \in \mathbb{C}^{N \times 1} \tag{3}$$

with

$$\mathbf{d}\big(u(t, \boldsymbol{\xi})\big) = \begin{bmatrix} D_{t,1}\big(u(t, \boldsymbol{\xi})\big) D_{r,1}\big(u(t, \boldsymbol{\xi})\big) e^{jku(t, \boldsymbol{\xi})d} \\ D_{t,2}\big(u(t, \boldsymbol{\xi})\big) D_{r,2}\big(u(t, \boldsymbol{\xi})\big) e^{j2ku(t, \boldsymbol{\xi})d} \\ \vdots \\ D_{t,N}\big(u(t, \boldsymbol{\xi})\big) D_{r,N}\big(u(t, \boldsymbol{\xi})\big) e^{jNku(t, \boldsymbol{\xi})d} \end{bmatrix}$$

The common phase multiplier represents the conventional azimuth chirp used for azimuthal SAR compression. The vector $\mathbf{d}(u)$ is commonly called Direction-of-Arrival (DOA)-vector.

The expected signal from a clutter point with reflectivity $p(t_b)$ located at azimuth position $x_b = v_a t_b$ can be also be described via (3) when $\boldsymbol{\xi}_0 = [1, 0, 0, t_b]$. Integration over all possible clutter contributions yields

$$\mathbf{c}(t) = \int p(t_b)\; \mathbf{s}_0\big(u(t - t_b, \boldsymbol{\xi}_0)\big)\; dt_b, \tag{4}$$

which corresponds to the convolution $\mathbf{c}(t) = (p \star \mathbf{s}_0)(t)$, when $p(\cdot)$ is considered the reflectivity function of the underlying scene and $\mathbf{s}_0(\cdot) = \mathbf{s}(\cdot, \boldsymbol{\xi}_0)$. Modeling the reflectivity as a stationary stochastic process (i.e. homogeneity), the composite clutter is fully described via its matrix-valued covariance function. The spectral density function of the linearly filtered clutter process $\mathbf{c}(t)$ at Doppler frequency f reads

$$\mathbf{R}(f) = \mathbf{R}_c(f) + \mathbf{R}_n(f) = \sigma_c^2 \mathbf{S}_0(f, \boldsymbol{\xi}) \mathbf{S}_0(f, \boldsymbol{\xi})^* + \sigma_n^2 \mathbf{I},$$

in which σ_c^2 represents the clutter power level, and $\mathbf{S}_0(f, \boldsymbol{\xi})$ is the Fourier transform of the clutter vector. Inevitable additive thermal noise, independent between channels, has been modeled as a stationary vector process with power spectral matrix $\mathbf{R}_n = \sigma_n^2 \mathbf{I}$. If the time base for the Fourier transform is sufficiently large, the random vectors at all Doppler bins become mutually independent; in other words the combined clutter vector along K frequency bins possesses a large spectral density matrix of block-diagonal structure, cf. (8).

2.1 Arbitrary antenna pattern

As mentioned earlier, the number of Rx channels L is usually much smaller than N, particularly for space based systems due to weight, power and cost restrictions. The analog combining and switching network in the front-end of the antenna can be modeled as a transformation or beamforming vector $\mathbf{t} \in \mathbb{C}^{N \times 1}$, such that the input of the l-th Rx channel (i.e. the effective one-way antenna pattern of this channel) is given as the product $\mathfrak{D}_{r,l}\big(u(t)\big) = \mathbf{t}_{r,l}^* \mathbf{d}\big(u(t)\big)$. Analogously, the Tx pattern is defined as $\mathfrak{D}_t\big(u(t)\big) = \mathbf{t}_t^* \mathbf{d}\big(u(t)\big)$. For MODEX-1 the normalized beamformers are given as $\mathbf{t}_t = \frac{1}{N}[1, \ldots, 1]' = \frac{1}{N}\mathbf{1_N}$ and $\mathbf{t}_{r,1} = \sqrt{\frac{2}{N}}[\mathbf{1_{N/2}}, \mathbf{0_{N/2}}]$.

2.2 Antenna Toggling/Switching

The concept of spatial diversity, in which both the Tx and Rx antenna pattern are modified between subsequent pulses has been recently proposed as a means to increase the target parameter estimation performance [2, 3]. In principle, switching changes the aperture partitioning from pulse to pulse (i.e., attenuating or turning off different TR-modules), eventually omitting contributions of some elements over time (the term toggling refers commonly to the modification of the Tx aperture). In order to keep it practical, the switching is usually done in a cyclic way by repeating the same sequence of partitions. From now on let us assume a cycle length of two, e.g. R2, the two parallel Rx outputs for every even pulse number are then combined with the two outputs of the previous odd-sampled output to create a four-dimensional signal vector. Obviously, this re-arranging of the data increases the effective pulse repetition interval by a factor of two. In other words, the spatial diversity has been traded off with a loss of effective unambiguous pulse repetition frequency (PRF). This procedure creates different antenna pattern with the potential of improving the GMTI performance.

Mathematically, the switching and toggling can be described as transformation matrices comprising the beamformer vectors for the different pulses. Preferably, the transformation matrices are chosen to be regular,

i.e. $\mathbf{T}_r^*\mathbf{T}_r = \mathbf{I}$, in order not to amplify the noise power levels. The corresponding antenna pattern for a two cycle switching/toggling scenario are

$$\begin{aligned}\boldsymbol{\mathfrak{D}}_t\big(u(t)\big) &= \mathbf{T}_t^*\mathbf{d}\big(u(t)\big) \in \mathbb{C}^{2\times 1}\\ \boldsymbol{\mathfrak{D}}_r\big(u(t)\big) &= \mathbf{T}_r^*\mathbf{d}\big(u(t)\big) \in \mathbb{C}^{4\times 1}.\end{aligned} \tag{5}$$

This general way of describing the individual antenna pattern conveniently avoids the computation of beamwidths, phase center locations or gain losses caused by the element tapering.

3 SNIR-optimum detection

3.1 Test problem

To test for the presence of a moving target in clutter plus noise, the following test problem (composite hypothesis) shall be considered:

$$\begin{aligned}\mathrm{H} &: \; Z(\mathbf{f}) = \mathbf{S}(\mathbf{f},\boldsymbol{\xi}) + \mathbf{C}(\mathbf{f}) + \mathbf{N}\\ \mathrm{A} &: \; Z(\mathbf{f}) = \mathbf{C}(\mathbf{f}) + \mathbf{N},\end{aligned} \tag{6}$$

with the real parameter vector $\boldsymbol{\xi} = [\alpha, \varphi, v_x, v_s, t_b]'$, given that $a = \alpha\exp(\varphi)$. Using the expressions in (5) and the method of stationary phase, the moving target signal vector in the Doppler domain can be computed to

$$\begin{aligned}\mathbf{S}(f,\boldsymbol{\xi};\mathbf{T}_t,\mathbf{T}_r) &= a\sqrt{\tfrac{j\lambda R_b}{2v_{\mathrm{rel}}^2}}e^{-j2kR_b\left(1-\frac{\lambda^2}{8v_{\mathrm{rel}}^2}\left(f+\frac{2v_s}{\lambda}\right)^2\right)}\\ &\times\big(\boldsymbol{\mathfrak{D}}_t\big(u(f)\big)\otimes[1,1]'\big)\odot\boldsymbol{\mathfrak{D}}_r\big(u(f)\big)\,e^{-2\pi f t_b},\end{aligned} \tag{7}$$

where $u(f,\boldsymbol{\xi}) = \frac{\lambda}{2v_a}\left(f - \frac{2v_s}{\lambda}\right)$, and $\otimes$ and $\odot$ denote the Kronecker and Hadamard products, respectively. Assuming K Doppler frequency samples, we may model the measured signal plus interference as Gaussian, i.e.

$$\mathbf{Z}(\mathbf{f},\boldsymbol{\xi}) \sim \mathcal{N}_{\mathbb{C}}^{4K}\left(\begin{bmatrix}\mathbf{S}(f_1,\boldsymbol{\xi})\\ \mathbf{S}(f_2,\boldsymbol{\xi})\\ \vdots\\ \mathbf{S}(f_K,\boldsymbol{\xi})\end{bmatrix}, \begin{bmatrix}\mathbf{R}(f_1) & \mathbf{0} & \cdots & \mathbf{0}\\ \mathbf{0} & \mathbf{R}(f_2) & \mathbf{0} & \vdots\\ \vdots & \mathbf{0} & \ddots & \mathbf{0}\\ \mathbf{0} & \cdots & \mathbf{0} & \mathbf{R}(f_K)\end{bmatrix}\right). \tag{8}$$

3.2 Test statistic

The Maximum Likelihood Quotient (MLQ) test reads:

$$\Lambda(\mathbf{Z}) = \underset{\boldsymbol{\xi}}{\operatorname{argmax}}\left\{\frac{f_{\mathbf{Z}}(\mathbf{z},\boldsymbol{\xi},\mathrm{H})}{f_{\mathbf{Z}}(\mathbf{z},\mathrm{A})}\right\} \gtrless \eta, \tag{9}$$

where $f_{\mathbf{Z}}(\cdot)$ denotes the Gaussian pdf and η the detection threshold. Taking the logarithm and maximization with respect to the complex amplitude a leads essentially to the test [3]:

$$\underset{v_x,v_s,t_b}{\arg\max}\Bigg|\underbrace{\sum_k \overbrace{\bar{\mathbf{S}}(f_k,v_x,v_s)^*}^{\text{De-chirping/ beamforming}}\;\underbrace{\mathbf{R}(f_k)^{-1}}_{\text{Clutter suppression}}\;\overbrace{\mathbf{Z}(f_k)}^{\text{Data in Doppler}}\;e^{-j2\pi f_k t_b}}_{\text{Discrete Fourier Transform}}\Bigg|^2.$$

For each Doppler frequency bin k, the clutter in the measured data vector is suppressed by application of the inverse covariance matrix, then de-chirped and summed over the channels using a matched filter bank $\mathbf{S}$ with varying velocity parameters. The resulting frequency samples are subsequently Fourier-transformed into the time domain, the location of the maximum peak sought and finally compared to η. Hence the name integrated or imaging STAP (iSTAP) [3]. The optimum achievable SNIR for iSTAP given a perfectly matched signal becomes:

$$\mathrm{SNIR}_{\mathrm{opt}}(v_{x,s},\mathbf{T}_{t,r}) = |a|^2\sum_k \mathbf{d}(f_k,\boldsymbol{\xi})^*\mathbf{R}(f_k)^{-1}\mathbf{d}(f_k,\boldsymbol{\xi}).$$

4 Optimum estimation, CRB

The variance of any unbiased estimator is larger or equal to the CRB. For the model (6) under the hypothesis with the unknown parameter vector $\boldsymbol{\xi}$, and Gaussian interference with covariance matrix given in (8), the elements of the Fisher information matrix $\mathbf{J}$ for the estimation of $\boldsymbol{\xi}$ are given by

$$\begin{aligned}J_{\mu\nu} &= \mathrm{E}\left[\frac{\partial}{\partial\boldsymbol{\xi}_\mu}\ln f_{\mathbf{Z}}(\mathbf{z},\boldsymbol{\xi})\frac{\partial}{\partial\boldsymbol{\xi}_\nu}\ln f_{\mathbf{Z}}(\mathbf{z},\boldsymbol{\xi})\right]\\ &= 2\Re\left\{\sum_k \mathbf{S}_\mu(f_k,\boldsymbol{\xi})^H\mathbf{R}(f_k)^{-1}\mathbf{S}_\nu(f_k,\boldsymbol{\xi})\right\},\end{aligned} \tag{10}$$

where $\mathbf{S}_\mu(f_k,\boldsymbol{\xi})$ is the derivative of the DOA-vector at frequency f_k with respect to parameter μ. Then $\mathrm{var}(\boldsymbol{\xi}_\mu) \geq (\mathbf{J})^{-1}_{\mu\mu}$.

4.1 Minimizing the CRB

One question naturally arises: Is there an optimum GMTI mode for R2 using a two cycle toggling and switching? For instance, one cost function could try to minimize the integrated CRBs over all Doppler frequencies with respect to the transformation matrices

$$\underset{\mathbf{T}_t,\mathbf{T}_r}{\operatorname{argmin}}\;\sum_{k=1}^{K}\mathrm{var}\Big(\boldsymbol{\xi}_{v_s}\Big)(f_k,\boldsymbol{\xi},\mathbf{T}_r,\mathbf{T}_t), \quad \text{u.c.} \quad \mathbf{T}_r^*\mathbf{T}_r = \mathbf{I}.$$

In general this is an constrained optimization over 128 unknowns (16 attenuator settings between zero and one and 16 phase shifter settings for Tx and Tr over two pulses), see Fig. 1 bottom right. However, since R2 always works in saturation during Tx only 96 unknowns remain. A numerical global minimization with a Genetic Algorithm in MATLAB took 27 hours and the result is plotted in **Fig.** 3. The first 32 values are the Tx phase shifters settings for both pulses, the following 32 are the Rx magnitudes and the last 32 correspond to the Rx phases, respectively.

Fig. 4 demonstrates the antenna power pattern associated with these TR-settings. Since the settings are mirror-inverted between pulses, four distinct phase responses arise but only two distinct magnitude patterns.

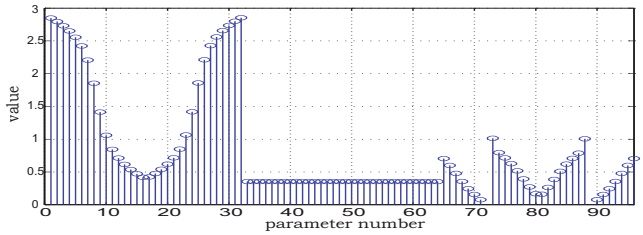

Figure 3: Optimum antenna tapering settings.

It is evident that the optimization demands slight opposite squints as well as that one pattern appears to be the derivative of the other. This is a property well known from the classic adaptive monopulse estimation of DOA angles.

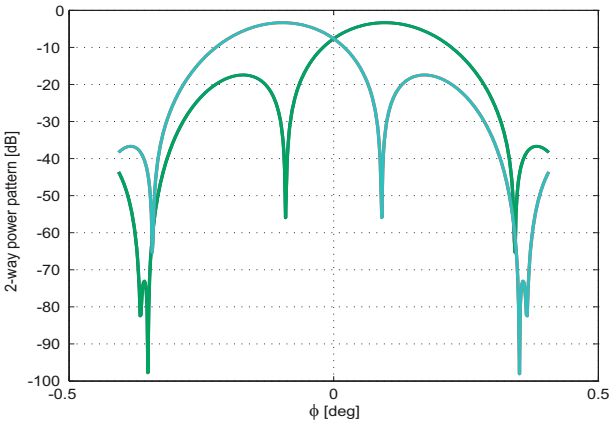

Figure 4: Antenna power pattern for optimized CRB.

5 Numerical results

Due to limited space and also to be able to compare results with those published in [2], simulation parameters have been set to $K = 256$ samples and a CNR=SNR=25 dB. The considered time base is small enough to consider $u(t) = u_t$ as constant so that the target's energy will be concentrated in a single Doppler cell $f_t = \frac{2v_a}{\lambda}(u_t + v_s/v_a)$. Therefore, no integration over Doppler cells is required and this case is usually dubbed factored STAP.

Fig. 5 compares the optimum SNIR for the four different GMTI modes. Obviously any tapering results in a SNR loss, which in this case lies somewhere between the 1/2 and 3/4 toggling modes.

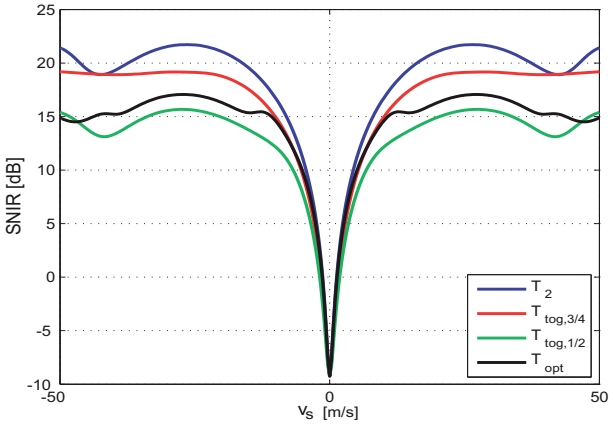

Figure 5: Optimum SNIR at $v_x = 0$.

The significant gain on the location estimation accuracy can be seen in **Fig.** 6, where the CRB is plotted for given $v_x = 0$ versus varying range velocities. The proposed mode not only reduces the peak error by more than one km compared to MODEX-1 (T_2) but is also about 400 m better than the currently best 3/4 toggle mode. It has been verified that these improvements hold for different v_x.

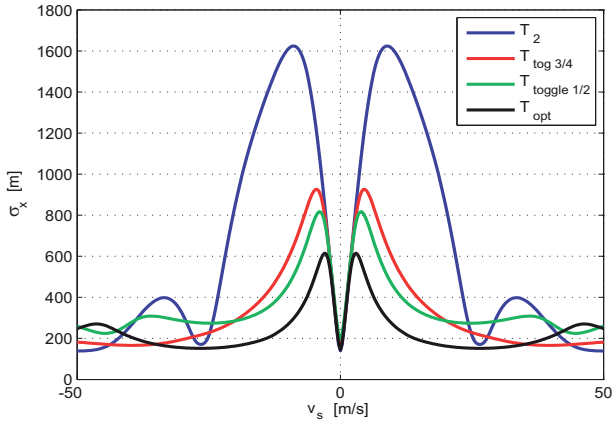

Figure 6: CRB for azimuth position at $v_x = 0$.

6 Conclusions

It has been shown that the positioning accuracy of moving targets can be considerably improved using phase and amplitude tapering in combination with aperture switching between subsequent pulses. The inevitable SNIR loss appears tolerable. One remarkable conclusion is that one shall drop the notions of phase centers and DPCA-condition as decisive GMTI factors even for two-channel systems. Unfortunately, the proposed concept cannot be demonstrated on R2 due to intrinsic hardware design restrictions. The required TR-settings cannot be changed quickly enough (loaded from memory into the modules) within one PRF. Nevertheless, the next generation of phased array radars such as RCM in principle permit this, provided they will be equipped with two parallel Rx channels. Another open question is whether or not practical (implementable) parameter estimators exist that reach the presented theoretical CRB. First approaches and Monte-Carlo simulations show promising results.

References

[1] C. H. Gierull and C. Livingstone: *SAR-GMTI Concept for RADARSAT-2*, In Klemm, R., (Ed.), The Applications of Space-Time Processing, Stevenage, IEE Press, 2003.

[2] J. H. G. Ender, C. H. Gierull and D. Cerutti-Maori: *Improved Space-Based Moving Target Indication via Alternate Transmission and Receiver Switching* IEEE Trans. GRS, vol. 46(12), pp. 3960-3974, Dec. 2008.

[3] D. Cerutti-Maori, I. Sikaneta and C. H. Gierull *Optimum SAR/GMTI processing and its application to the radar satellite RADARSAT-2 for traffic monitoring* IEEE Trans. GRS, vol. 50(10), pp. 3868-3881, Oct. 2012.